ASSESSING THE INFLUENCE OF CRASH PULSE, SEAT FORCE CHARACTERISTICS, AND HEAD RESTRAINT POSITION ON NIC_{max} IN REAR-END CRASHES USING A MATHEMATICAL BioRID DUMMY

Linda Eriksson[1,2]
Ola Boström[3]

[1] Autoliv Sweden, Vårgårda, Sweden
[2] Department of Machine and Vehicle Design, Chalmers University of Technology, Sweden
[3] Autoliv Research, Vårgårda, Sweden

ABSTRACT

The major car and crash related risk factors for Whiplash Associated Disorders (WAD) 1-3 long-term neck injuries in rear-end crashes are the shape of the crash pulse, the seat-force characteristics and the head restraint position. However, the specific roles of these factors are not yet fully understood, which makes it difficult to find adequate countermeasures and to design protective car seats. In order to study these issues, a mathematical MADYMO model of the first version of the Biofidelic Rear Impact Dummy (BioRID I) has previously been developed. In addition, a neck injury criterion, NIC_{max}, has been proposed and evaluated by means of dummy, human and rear-end impact simulations. In this paper the MADYMO BioRID I and four car seats ranked differently according to a disability ranking list are used to study the influence of crash pulse, seat-force characteristics, and head restraint position on the NIC_{max} in rear-end crashes. A set of 64 crash pulses with four pulse shapes, a peak acceleration from 2.5 to 10g, and speed change (Δv) from 2 to 5 m/s were used. Also, 22 real-life rear-end crashes, where the duration of the occupants' symptoms were known, were used in the simulations.

The results showed a correlation between the NIC_{max} outcome and the disability ranking of the four seats. The critical parameters regarding the seat force characteristics were found to be the recliner torque stiffness and yield limit. The head restraint position had a major influence on the NIC_{max} for one of the four seats. Regarding the crash pulse, the speed change during the first 85 ms of the impact, $\Delta v_{85\,ms}$, equivalent to mean acceleration during the same time period, was shown to be the best NIC_{max} predictor. For the real-life crash-pulses the levels of NIC_{max}, and the $\Delta v_{85\,ms}$, correlated well to the duration of the occupants' symptoms.

THE SPEED CHANGE (Δv) and mean acceleration of the car are commonly used measures when estimating the severity of car crashes. According to Kullgren (1998) these measures are not suitable for relating impacts to injury outcome. Krafft et al. (1998) concluded from real-life rear-end crashes that short-term symptoms to the neck are strongly related to the Δv while long-term symptoms seemed to be more related to the acceleration. Jakobsson et al. (1999) showed, analysing Volvo crash data, that the risk of sustaining AIS 1 neck injuries remains fairly constant irrespective of the Equivalent Barrier Speed (EBS).

The complexity of the various human and car-crash related factors causing the broad set of symptoms included in the diagnosis of Whiplash Associated Disorders (WAD) 1-3 is tremendous. No single injury mechanism has so far been proposed as responsible for all the symptoms. However, a neck injury criterion, NIC_{max}, has been proposed as a measure of the effect of the violence to the neck, caused by a quick head-lag motion (Boström et al. 1996). This criterion is a result of a series of experiments on pigs, where pressure amplitudes in the spinal canal were found to correlate with nerve cell damage. Eichberger et al. (1999) later showed that a correlation between the NIC_{max} and pressure amplitudes in the spinal canal also applied to human subjects. Mechanical and mathematical simulations of rear-end impacts, have shown that NIC_{max} is sensitive to the major car and crash-related risk factors for neck injuries with long-term symptoms (Boström et al. 1997, Boström et al. 1998, Eichberger et al. 1998, Boström et al. 1999). Recently, the first version of the Biofidelic Rear Impact Dummy (BioRID I) was developed and presented (Davidsson et al. 1998). The BioRID I offers a significantly more human like head-neck performance compared to earlier crash-test dummies in rear-end crashes (Svensson et al. 1999).

The aim of this study was to assess the influence of crash pulse, seat force characteristics and head restraint position on the NIC_{max} in rear-end impacts. The method used was to simulate various rear-end crashes using a previously developed MADYMO model of the BioRID I and four seats with different disability ranking. A second aim was to verify the relevance of NIC_{max} by comparing results of mathematical simulations with real-life crash data.

METHOD

MADYMO MODELS – The study was designed to assess the influence of crash pulse, seat-force characteristics and head restraint position on the NIC_{max} in low velocity rear-end impacts, using MADYMO (TNO 1997) models of the Biofidelic Rear Impact Dummy, BioRID I, and four car seats. Eriksson (1999) developed the dummy and seat models and validated the models to sled-tests designed by Boström et al. (1999). The model set-ups and the validation methodology are found in the appendix. The seat models represented seats from good (G_1 and G_2) and bad (B_1 and B_2) cars according to a disability ranking list (Krafft 1998). Two crash pulses (Figure 1) with different peak accelerations and almost the same Δv were used.

The H-point of the MADYMO BioRID I was placed in the same position in the MADYMO seat models as the H-point of BioRID I was in the sled-tests. Similarly to the sled-tests, the baseline of the head was placed in a horizontal position. All seat backs were inclined 16° to the vertical. No seat belt was used in the MADYMO simulations. The NIC_{max} values were calculated according to Muser et al. (1998),

$$NIC_{max} = \text{maximum}_{\text{first 150 ms}}(a_{rel} \times 0.2 + v_{rel}^2) \qquad \text{(Equation 1)}$$

In Equation 1, a_{rel} and v_{rel} are the relative T1 to head acceleration and velocity, respectively. The T1 and head (centre of gravity) accelerations are the x-components for each local co-ordinate system according to SAE J211.

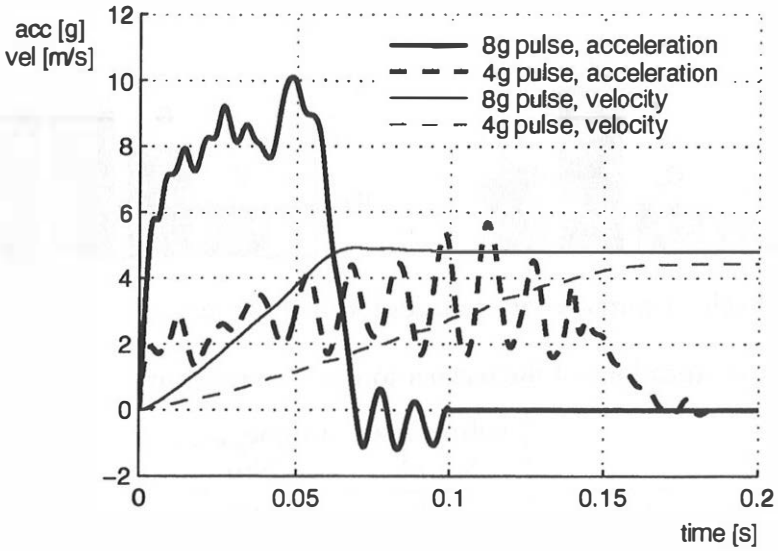

Figure 1. The crash pulses used in the validation sled-tests.

Eriksson (1999) showed that the head restraint position and the recliner torque characteristics, defined in Figure 2 and Table 1, mainly influenced the NIC_{max} outcome.

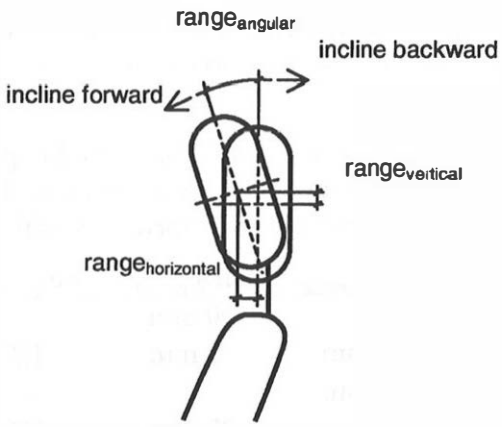

Figure 2. Head restraint position definitions.

Table 1. Recliner torque characteristics and head restraint geometry definitions.

$torque_{yield\ limit}$	Recliner yield limit torque.
$stiffness_{2-7°}$	The slope of the recliner torque stiffness in the interval from 2 to 7°.
$range_{horizontal}$	Horizontal difference between the most rearward and the most forward position of the centre of the head restraint.
$range_{vertical}$	Vertical difference between the lowest and the highest position of the centre of the head restraint.
$range_{angular}$	Angular adjusting range of the head restraint.

The recliner torque characteristics for the four seats are shown in Figure 3 and classified according to Table 2.

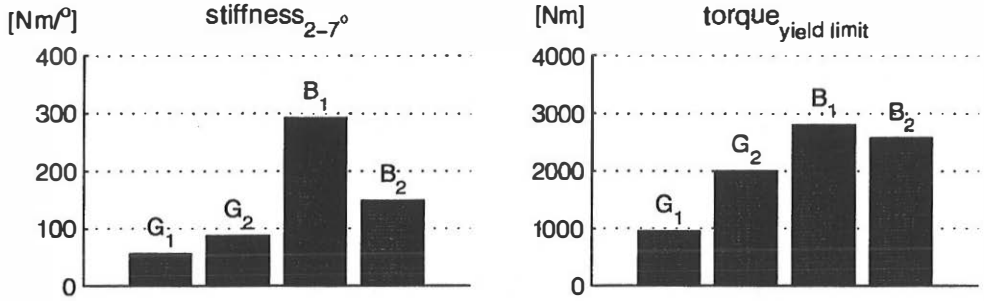

Figure 3. Recliner torque characteristics for the four seats.

Table 2. Classifications of the recliner torque characteristics.

	$stiffness_{2-7°}$ Nm/°	$torque_{yield\ limit}$ Nm
low	< 100	< 1000
medium	100-200	1000-2000
high	> 200	> 2000

To assess the influence of head restraint position, the head restraint was placed in two positions for each seat, corresponding to the adjustable range of the real seats. Position 1: the head restraint was inclined backward in the lowest and most rearward position, and, Position 2: the head restraint was inclined forward in the highest and most forward position. The differences between these positions are shown in Table 3 and Figure 4.

Table 3. Differences between the two head restraint positions: inclined backward in the lowest and most rear position (Position 1) and inclined forward in the highest and most forward position (Position 2).

seat	$range_{horizontal}$	$range_{vertical}$	$range_{angular}$
G_1	-	30 mm	-
G_2	14 mm	8 mm	12°
B_1	20 mm	-	-
B_2	33 mm	25 mm	25°

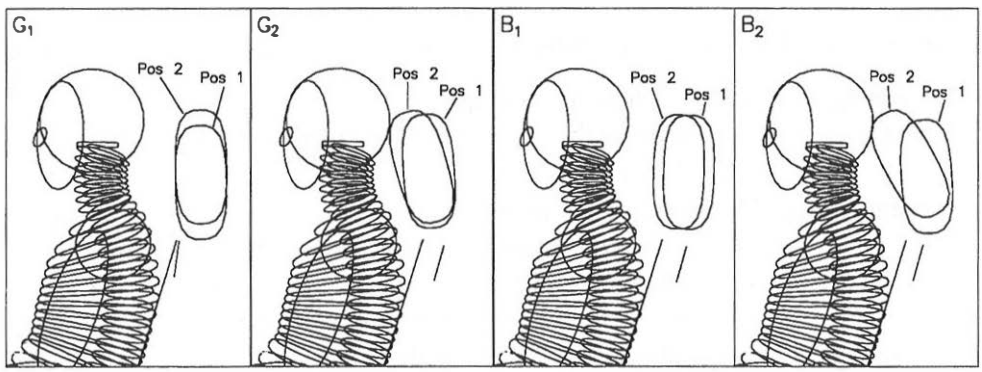

Figure 4. Head restraints in Position 1 and Position 2 for all seats.

CRASH PULSE PARAMETERS – In order to describe the relation between the NIC_{max} value and the crash pulse, the definitions in Table 4 and Figure 5 were used.

Table 4. Crash pulse definitions.

peak $acc_{tot\,pulse}$	Maximum acceleration during the whole crash pulse.
peak $acc_{x\,ms}$	Maximum acceleration during the first x ms of the crash pulse.
$\Delta v_{tot\,pulse}$	Velocity change for the whole crash pulse.
$\Delta v_{x\,ms}$	Velocity change up to x ms after the crash pulse started.
T	Duration of the crash pulse.

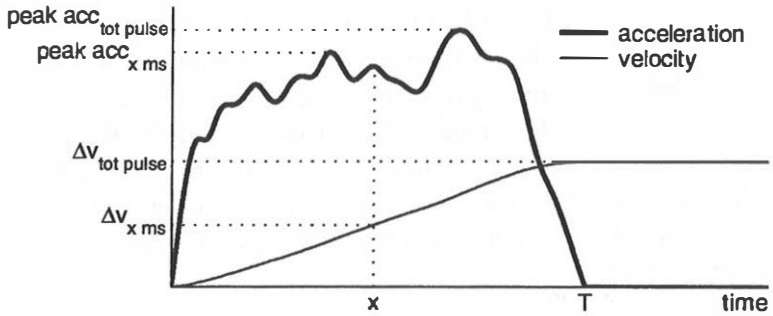

Figure 5. Crash pulse definitions.

The MADYMO models of the BioRID I and the four seats, with the head restraints in Position 1, were exposed to a set of 64 crash pulses. The varying crash pulse parameters were shape (Figure 6), peak $acc_{tot\,pulse}$ and $\Delta v_{tot\,pulse}$. Peak $acc_{tot\,pulse}$ varied between 2.5 and 10 g in steps of 2.5g, and $\Delta v_{tot\,pulse}$ varied between 2 and 5 m/s in steps of 1 m/s. The duration, T, for the combination of crash pulses where Δv = 2 and 5 m/s, and peak $acc_{tot\,pulse}$ = 2.5 and 10 g are given in Table 5.

Table 5. Duration, T, for some crash pulses.

$\Delta v_{tot\,pulse}$	2 m/s		5 m/s	
peak $acc_{tot\,pulse}$	2.5 g	10 g	2.5 g	10 g
sine-wave	128 ms	32 ms	320 ms	80 ms
superimposed sine-waves	167 ms	42 ms	419 ms	105 ms
square	82 ms	20 ms	204 ms	51 ms
degressive saw-tooth	163 ms	41 ms	408 ms	102 ms

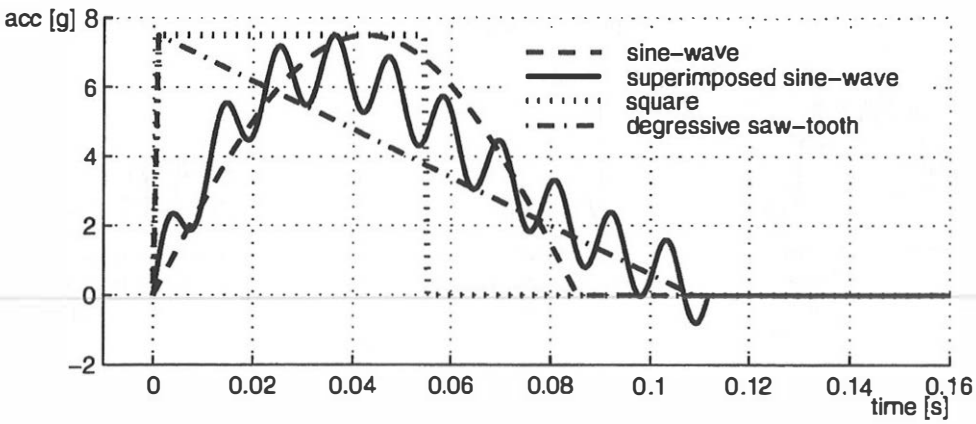

Figure 6. Definition of crash pulse shapes.

COMPARISON OF SEATS – In order to compare the seat force characteristics of the G_1, G_2, B_1, and B_2 seats, and to assess the influence of head restraint position, the MADYMO models of the BioRID I and the four seats, with the head restraints in Position 1 and Position 2, respectively, were exposed to the set of 64 crash pulses used in the crash pulse parameter study.

To evaluate the NIC_{max} outcome for the numerous simulations, the following ratio was used for different crash pulse sub-sets.

$$R_X = \frac{\#\text{ simulations with } NIC_{max} > X\ m^2/s^2 \text{ in the crash pulse sub-set}}{\#\text{ all simulations in the crash pulse sub-set}} \qquad \text{(Equation 2)}$$

COMPARISON WITH REAL-LIFE DATA – Krafft et al. (1998) reported 22 real-life rear-end crashes in which crash recorders were mounted in the cars, and where the duration of the occupants' symptoms were known. For six cases, labeled A to F, the crash pulses were recorded (Figure 7). For cases G to K, the peak accelerations were recorded as being between 2.7 and 4.3g. For the remaining 11 cases, L to V, the peak accelerations were too low to trigger the recorder, with trigger levels ranging between 2.4 and 3.3 g. Only the occupants in cases B and D sustained long-term symptoms (Krafft 1999).

The MADYMO BioRID I and the B_2 seat, with the head restraint in Position 1, were subjected to the six recorded real-life crash pulses. The reason for choosing the B_2 seat was that it most resembled the seats in the real cars (Krafft 1999). The NIC_{max} values and various crash pulse parameters were compared to the duration of the occupants' symptoms. For cases G to V, the NIC_{max} values were found using the linear regression in Figure 9 and an estimation of the maximum Δv_{85ms}.

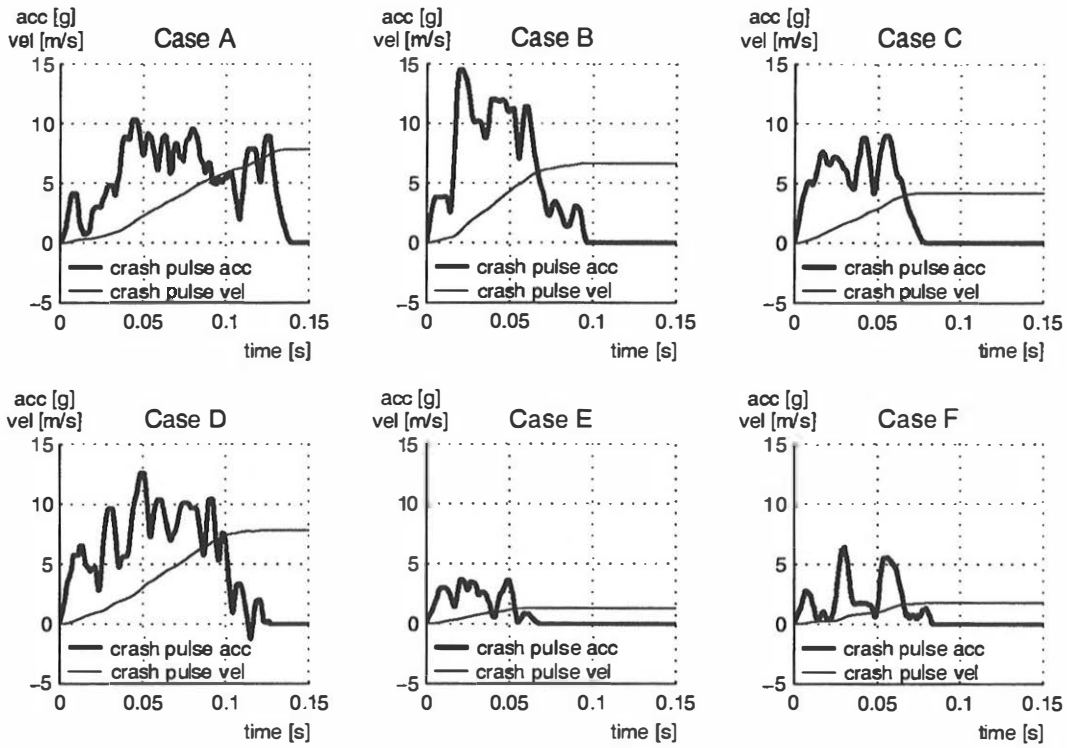

Figure 7. Real-life rear-end impact crash pulses (from Krafft et al. 1998).

RESULTS

CRASH PULSE PARAMETERS – In order to relate the NIC_{max} values to the crash pulse variables in Table 4, a regression analysis, linear least-squares fit, was performed for the crash pulse study with the head restraint in Position 1. Regarding $\Delta v_{tot\,pulse}$ and peak $acc_{tot\,pulse}$, the range of NIC_{max} and the squared correlation coefficients, r^2, are given in Table 6 and Table 7 for all seats. The squared correlation coefficients, r^2, for peak $acc_{x\,ms}$ and $\Delta v_{x\,ms}$ are given in Figure 8 for x between 0 and 150 ms.

Table 6. The minimal and maximal NIC_{max} values given in m^2/s^2 and the squared correlation coefficients from the regression analysis of NIC_{max} versus $\Delta v_{tot\,pulse}$, for constant $\Delta v_{tot\,pulse}$. Head restraints were in Position 1.

	2 m/s		3 m/s		4 m/s		5 m/s		corr. coef.
	min	max	min	max	min	max	min	max	r^2
G_1	6	7	7	13	6	17	5	16	0.00
G_2	4	8	7	11	7	16	7	27	0.36
B_1	8	14	9	22	10	34	9	30	0.30
B_2	7	12	8	17	9	27	7	27	0.31

Table 7. The minimal and maximal NIC_{max} values given in m^2/s^2 and the squared correlation coefficients from the regression analysis of NIC_{max} versus peak $acc_{tot\,pulse}$, for constant peak $acc_{tot\,pulse}$. Head restraints were in Position 1.

	2.5g		5g		7.5g		10g		corr. coef.
	min	max	min	max	min	max	min	max	r^2
G_1	5	11	6	17	5	13	6	16	0.03
G_2	4	7	7	19	6	27	6	27	0.29
B_1	8	12	12	21	13	30	13	34	0.40
B_2	7	12	11	22	11	26	11	27	0.41

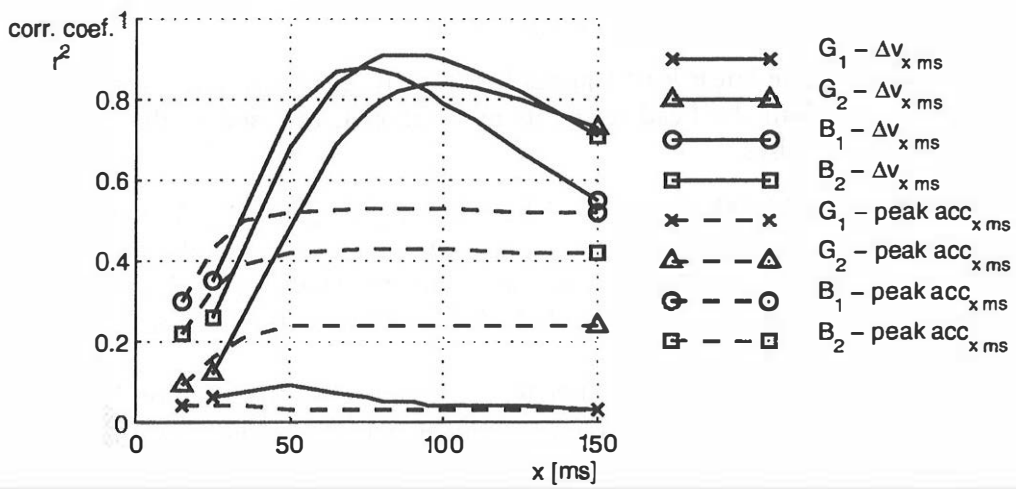

Figure 8. The squared correlation coefficients from the regression analysis corresponding to the NIC_{max} values versus peak $acc_{x\,ms}$ and $\Delta v_{x\,ms}$, respectively, x ranged from 0 to 150 ms. Head restraints were in Position 1.

It was found that $\Delta v_{x\,ms}$ was a good predictor for NIC_{max} values in an interval of x from around 70 ms to 110 ms for the G_2, B_1, and B_2 seats. However, $\Delta v_{tot\,pulse}$, peak $acc_{tot\,pulse}$ and peak $acc_{x\,ms}$ were no good predictors. The NIC_{max} values for seat G_1 were low for all crash pulses and showed no correlation with any of the measured quantities of the crash pulses. For all seats, the NIC_{max} values versus $\Delta v_{85\,ms}$ are given in Figure 9, the linear least-squares fits are indicated.

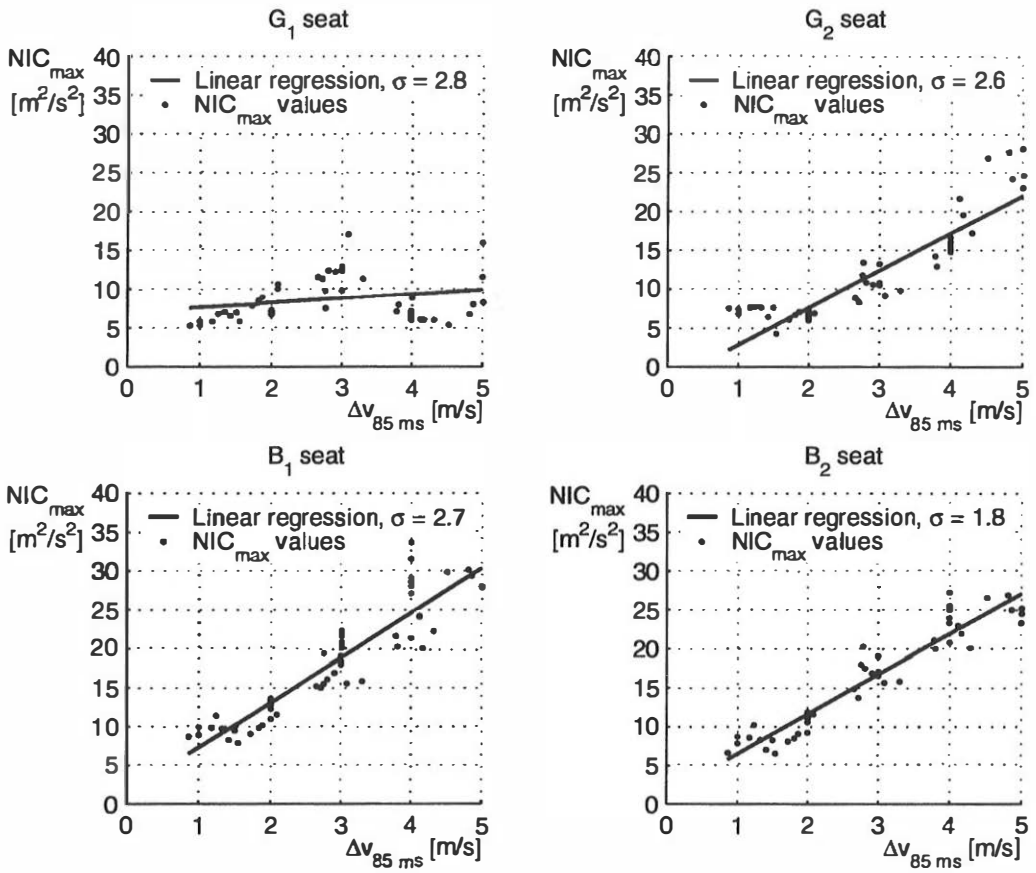

Figure 9. The linear least-squares fits for NIC_{max} versus $\Delta v_{85\,ms}$ for the four seats, with the head restraints in Position 1, exposed to the set of 64 crash pulses.

COMPARISON OF SEATS – The ratios R_{10}, R_{15}, and R_{20}, (Equation 2), for the crash pulse sub-sets with $\Delta v_{tot\,pulse}$ = 2, 3, 4, and 5 m/s with the head restraints in Position 1 and Position 2 are shown in Figure 10. The G seats showed considerably lower ratios in the simulations with NIC_{max} > 15 and 20 m^2/s^2 for $\Delta v_{tot\,pulse}$ < 5 m/s compared to the B seats.

Taking into account the recliner torque characteristics in Figure 3 and classification in Table 2, for head restraints in Position 1, low recliner $stiffness_{2\text{-}7°}$ and low recliner torque yield limit (G_1 seat) resulted in R_{15} and R_{20} ratios less than 0.1 for all $\Delta v_{tot\,pulse}$. High recliner $stiffness_{2\text{-}7°}$ and high recliner torque yield limit (B_1 seat) resulted in $R_{15}$and R_{20}ratios less than 0.1 only for $\Delta v_{tot\,pulse}$ = 2 m/s. Low recliner $stiffness_{2\text{-}7°}$ and high recliner torque yield limit (G_2 seat) resulted in R_{15} ratios less than 0.1 for $\Delta v_{tot\,pulse} \leq$ 3 m/s, and R_{20} ratios less than 0.1 for $\Delta v_{tot\,pulse} \leq$ 4 m/s. Medium recliner

stiffness$_{2.7°}$ and high recliner torque yield limit (B_2 seat) resulted in R_{15} ratio less than 0.1 only for $\Delta v_{tot\ pulse}$ = 2 m/s, and R_{20} ratios less than 0.1 for $\Delta v_{tot\ pulse} \leq 3$ m/s.

The main differences between the two head restraint positions were found for the B_2 seat, where the R_{10}, R_{15}, and R_{20} ratios, summed for all crash pulses, decreased by 35%, 76%, and 88%, respectively.

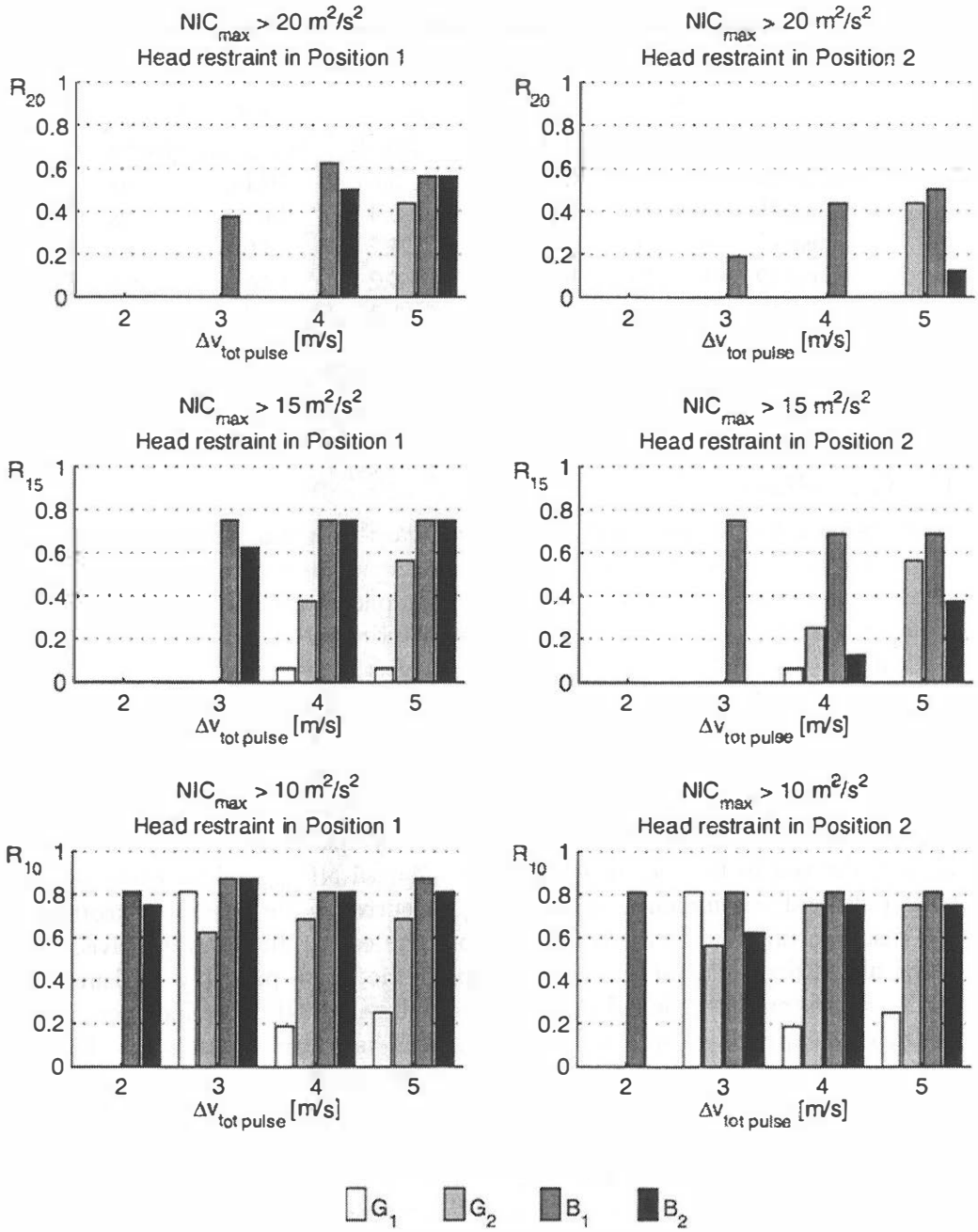

Figure 10. Comparison between the four seats in terms of the ratios R_{10}, R_{15}, and R_{20}, for the crash pulse sub-sets with $\Delta v_{tot\ pulse}$ = 2, 3, 4, and 5 m/s with the head restraints in Position 1 and Position 2.

COMPARISON WITH REAL-LIFE DATA – For the real-life crash pulses, the NIC_{max} values for the B_2 seat, $\Delta v_{tot\ pulse}$, $\Delta v_{85\ ms}$, peak $acc_{tot\ pulse}$, and the duration of the occupants' symptoms are shown in Table 8. The simulations of the cases where the occupants sustained long-term symptoms, cases B and D, compared to the other cases, showed considerably higher NIC_{max} values (around 40 m^2/s^2) as well as $\Delta v_{85\ ms}$ (> 6 m/s).

Table 8. NIC_{max} values for the B_2 seat, with the head restraint in Position 1, subjected to the real-life crash pulses in cases A to F, and estimated NIC_{max} values from the crash pulse study for cases G to V.

	NIC_{max} [m^2/s^2]	$\Delta v_{tot\ pulse}$ [m/s]	$\Delta v_{85\ ms}$ [m/s]	peak $acc_{tot\ pulse}$	long-term symptoms
Case A	24	7.8	5.0	10.1 g	no
Case B	45	6.5	6.4	14.7g	yes
Case C	26	4.1	4.2	9.0g	no
Case D	39	7.2	6.2	12.6g	yes
Case E	7	1.2	1.3	3.7g	no
Case F	9	1.7	1.8	6.1g	no
Case G-K	< 20		< 3.6	< 4.3g	no
Case L-V	< 14		< 2.4	< 3.3g	no

DISCUSSION

A strength of the mathematical models used was the relation to real physical counterparts (dummy and seats), which enabled a comparison with real-life crash data. The dummy used was the BioRID I designed to replicate the human relative motion of the head to torso and allowing a correct calculation of NIC_{max}.

Krafft et al. (1998) showed that the shape of real-life crash pulses varies to a large extent and that the total speed change, $\Delta v_{tot\ pulse}$, is not a good measure to predict the duration of the occupants' symptoms. The present study showed that total speed change and peak acceleration were no good NIC_{max} predictors. Rather, speed change during a limited time period, 70 to 110 ms, of the impact, equivalent to mean acceleration during the same time period, showed to predict high NIC_{max} values well. The G_1 seat showed to be tolerant in the sense that all NIC_{max} values were low and the crash pulse did not influence much. NIC_{max} occurred in the time range from 65 ms to 150 ms. The time lag of the response from the car to the dummy pelvis, from the pelvis along the spine of the dummy up to the head, probably explains why the NIC_{max} value can be predicted a time period before the NIC_{max} value occurs.

The cars exposed to the real-life crash pulses had seats similar to the B_2 seat. For this seat, the NIC_{max} values for the crash pulses which led to long-term symptoms were 39 and 45 m^2/s^2, considerably higher compared to the values for the 20 crash pulses which did not lead to long-term symptoms. For the crash pulse set of 64 pulses, the B seats, compared to the G seats, generated substantially more NIC_{max} values above a level of 15 as well as 20 m^2/s^2. Human factors such as psychic, socio-economic and therapeutic factors are also likely to influence the injury outcome. Therefore, it must be noted that a crash pulse leading to a high NIC_{max} value in this study does not necessarily lead to a neck injury in a real-life crash.

The fact that the G_2 seat performance was comparable with that of the B seats for $\Delta v_{tot\ pulse}$ = 5 m/s, but not for lower speed changes, would seem to indicate that the Δv of the "average" rear-end impact leading to long-term symptoms could be less

than 5 m/s (18 km/h). An alternative explanation could be that the rear-end structure of the G_2 car model was very soft.

The difference between the head restraint Position 1 and Position 2 slightly influenced the NIC_{max} outcome for the G_1, G_2 and the B_1 seats. For the B_2 seat, the change in head restraint position considerably influenced the NIC_{max} outcome. The head restraint on the B_1 seat was only adjustable 20 mm in the horizontal direction, which was a too small adjustment to lower the NIC_{max} values. The head restraint on the B_2 seat had an angular adjustment, which was crucial for reducing the distance between the head and the head restraint when the seat back inclined backwards.

The MADYMO models used in this study have proven useful for evaluating the initial head-lag phase in rear-end impacts. The number of seats, the variety of crash pulses and other dummy evaluation parameters than NIC_{max} (for example neck forces and moments) can be incorporated in future studies.

CONCLUSION

The MADYMO BioRID I response on NIC_{max} in rear-end collisions was evaluated for four seats ranked differently according to a disability ranking list. According to the MADYMO simulations:

- For the B (bad) seats, $\Delta v_{85\,ms}$ correlated well ($r^2 > 0.75$) with NIC_{max}, in contrast to peak acceleration and total speed change ($\Delta v_{tot\,pulse}$).
- The incidences of NIC_{max} above 15 and 20 m^2/s^2 were much higher for the B (bad) seats compared with the G (good) seats.
- Low recliner torque yield limit (< 1000 Nm), and low recliner $stiffness_{2\text{-}7°}$ (< 100 Nm/°), resulted in low NIC_{max} values for all $\Delta v_{tot\,pulse}$.
- Adjusting the head restraint to the highest and most forward position, and inclining it forward, lowered NIC_{max} considerably for the B_2 seat.
- For the set of real-life crash pulses, the NIC_{max} values correlated well with the duration of the occupants' symptoms.

The results verified the relevance of using NIC_{max} as a predictor of neck injuries with long-term symptoms. NIC_{max} and the MADYMO models of the BioRID I and the seats were shown to be good tools for assessing the effect of violence associated with the initial relative head to torso motion in rear-end crashes.

ACKNOWLEDGEMENT

Thanks are due to Yngve Håland, Autoliv Research, and Christine Räisänen, Chalmers University of Technology, who provided us with helpful comments on the language and structure of this paper. This study was part of the Swedish Vehicle Research Program and was administrated by NUTEK, Sweden.

REFERENCES

Boström O.; Svensson M.Y; Aldman B.; Hansson H.A.; Håland Y.; Lövsund P.; Seeman T.; Suneson A.; Säljö A.; Örtengren T. (1996): A new Neck Injury Criterion Candidate-Based on Injury Findings in the Cervical Spinal Ganglia after Experimental Neck Extension Trauma. IRCOBI, Dublin, Ireland, pp. 123-136.

Boström O.; Krafft M.; Aldman B.; Eichberger A.; Fredriksson R.; Håland Y.; Lövsund P.; Steffan H.; Svensson M.Y.; Tingvall C. (1997): Prediction of Neck Injuries in Rear Impacts Based on Accident Data and Simulations. IRCOBI, Hannover, Germany, pp. 251-264.

Boström, O.; Fredriksson, R.; Håland, Y.; Svensson, M.Y.; Mellander, H. (1998): A sled test procedure proposal to evaluate the risk of neck injury in rear impacts using a new neck injury criterion (NIC). 16th ESV Conference, Windsor, Canada, pp. 1579-1585.

Boström O.; Fredriksson R.; Håland Y.; Jakobsson L.; Krafft M.; Lövsund P.; Muser M.H.; Svensson M.Y. (1999): Comparison of Car Seats in low Speed Rear-End Impacts Using the BioRID Dummy and the new Neck Injury Criterion (NIC). To be published in Accident Analysis and Prevention, special issue.

Davidson J.; Svensson M.Y.; Flogård A.; Håland Y.; Jakobsson L.; Linder A.; Lövsund P.; Wiklund K. (1998): BioRID I – A new Biofidelic Rear Impact Dummy. IRCOBI, Göteborg, Sweden, pp. 377-390.

Eichberger A.; Darok M.; Steffan H.; Leinzinger P.E.; Svensson M.Y.; Boström O. (1999): Pressure Measurements in the Spinal Canal of Post-Mortem Human Subjects during Rear-End Impact and Correlation of Results to the Neck Injury Criterion (NIC). To be published in Accident Analysis and Prevention, special issue.

Eriksson L (1999): Mathematical Models of the BioRID I and Four Car Seats. Manuscript.

Jakobsson L.; Lundell B.; Norin H.; Isaksson-Hellman I. (1999): WHIPS – Volvo´s Whiplash Protection Study. To be published in Accident Analysis and Prevention, special issue.

Krafft M. (1998): A comparison of short and long-term consequences of AIS 1 neck injuries, in rear impacts. IRCOBI, Göteborg, Sweden, pp. 235-248.

Krafft, M.; Kullgren, A.; Tingvall, C. (1998): Crash pulse recorders in rear impacts - real life data. 16th ESV Conference, Windsor, Canada, pp 1256-1262.

Krafft M. (1999): Personnel communication.

Kullgren, A (1999): Validity and reliability of vehicle collision data. Doctoral Thesis, Karolinska Institutet, Stockholm, Sweden.

Muser et al. (1998): http://www.biomed.ee.ethz.ch

Svensson M.Y.; Boström O.; Davidsson J.; Hansson H.A.; Håland Y.; Lövsund P.; Suneson A.; Säljö A. (1999): Neck Injuries in Car Collisions – a Review Covering a Possible Mechanism and the Development of a new Rear-Impact Dummy. To be published in Accident Analysis and Prevention, special issue.

TNO Road Vehicles Research Institute (1997): MADYMO Theory Manual 3D and User's Manual 3D, version 5.3. Delft, The Netherlands.

APPENDIX

This appendix gives a brief description of the model set-ups and the validation methodology of the MADYMO BioRID I and the four car seats used in this study.

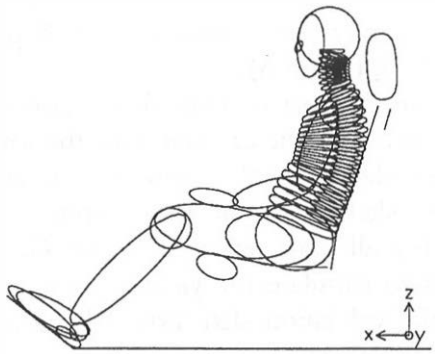

Figure A. The MADYMO BioRID I and the G_2 seat.

BioRID I – A three dimensional mathematical model of the mechanical BioRID I (Davidsson et al.) was developed by Eriksson (1999) in MADYMO (TNO 1997). The MADYMO BioRID I head is the same as the MADYMO Hybrid III (TNO 1997) head and connected to the C1 vertebra by a pin joint. The MADYMO spine model consists of 7 cervical (C1-C7), 12 thoracic (T1-T12), and 5 lumbar (L1-L5) vertebrae connected by pin joints, as in the physical counterpart. The L5 vertebra is connected to the pelvis by a pin joint. The joint-to-joint centre distances, the range of motions, and the curvature of the MADYMO spine are equal to the mechanical BioRID I (Davidsson et al. 1998). The static joint torque in the MADYMO BioRID I spine are equal to the mechanical BioRID I static joint torque (Davidsson et al. 1998). The damping stiffness in the MADYMO spine joints are estimated to correspond to the damping of polyurethane rubber blocks in the physical counterpart. The cables in the neck in the mechanical BioRID I are not in the MADYMO model, since the cables only influence the kinematics slightly during the first 150 ms of the impact.

The torso (chest and abdomen) of the mechanical BioRID I is moulded out of soft silicon rubber (Davidsson et al. 1998). To give the MADYMO BioRID I the same surface contour as the physical counterpart, the MADYMO torso is modelled by bodies attached to the vertebrae. Kelvin elements, in a line along the sagittal plane, connect the bodies to each other and to the pelvis. The shoulder joints are attached to a scapula-clavicle structure moulded into the silicon rubber in the mechanical BioRID I. The shoulder joints in the MADYMO BioRID I are, via clavicles, connected to the T1 vertebra and their joint stiffness is estimated to correspond to that of the physical counterpart. The arms in the MADYMO BioRID I are the same as in the MADYMO Hybrid III.

The legs of the mechanical BioRID I are the same as the mechanical Hybrid III (Davidsson et al. 1998) and therefor the legs of the MADYMO Hybrid III have been used in the MADYMO BioRID I. The weight and the geometry of the MADYMO BioRID I pelvis and the MADYMO BioRID I hip joint stiffness correspond to the physical counterpart. The MADYMO BioRID I has the same mass distribution as the physical counterpart. Inertia of the head, legs and arms are equal to the MADYMO Hybrid III. The inertia of the spine and torso were calculated and adjusted to correspond to the validation sled-tests.

SEATS – Mathematical models of four car seats were developed by Eriksson (1999) in MADYMO (TNO 1997). The seat models represented seats from good (G_1 and G_2) and bad (B_1 and B_2) cars according to a disability ranking list (Krafft 1998).

All MADYMO seats have the same geometry, with the exception of the placements of the upper beam and the head restraint. All seats have the same mass and inertia. The MADYMO seats are three dimensional, but all parts are flat in the y-direction (sled co-ordinate system, Figure A).

The MADYMO seat cushions consist of two planes corresponding to the seat cushion padding, and one cylinder for the contact with the lower legs. The contact stiffness characteristics of the planes are the same for all seats and estimated to correspond to the validation sled-tests. For the cylinder, the contact stiffness characteristics are the same for all seats, except for the G_1 seat which has been given different characteristics to simulate the yielding seat cushion structure, and estimated to correspond to the validation sled-tests. All parts of the seat cushion are fixed to the sled co-ordinate system.

The MADYMO seat back consists of a stiff seat back frame with three planes corresponding to the seat back padding, one plane corresponding to the upper beam, and one cylinder corresponding to the head restraint. The stiff seat back frame is connected to the seat cushion by a joint (corresponding to the seat recliner) with two degrees of freedom: translation along the sled x-axes, and rotation around the sled y-axes. These joints have the same initial placement and incline for all seats. The three planes, corresponding to the seat back padding, have different contact stiffness and damping characteristics. For each seat, the contact stiffness characteristics at two positions on the seat backs have been measured and implemented in the MADYMO seat models. For each seat, the upper beam and head restraint were placed to correlate to the measured placements. The contact stiffness characteristics for the upper beams and the head restraints have been estimated. The contact damping characteristics and friction coefficients have been estimated for all seats to correlate to the validation sled-tests. The static torque of all recliner joints have been measured and implemented in the MADYMO seat models. For each seat, the static recliner joint torque has been adjusted, and the damping characteristic has been estimated, to correspond to the validation sled-tests.

VALIDATION – The MADYMO BioRID I and the four MADYMO seat models were validated to sled-tests (Boström et al. 1999) with two crash pulses (Figure 1). In the sled-tests the head, T1, and pelvis accelerations, according to SAE J211, were measured in the BioRID I. For the seats, the recliner x-displacement and y-rotation were measured.

Results from the MADYMO simulation and the validation sled-tests are given in Figure B for the G_1 seat, Figure C for the G_2 seat, Figure D for the B_1 seat, and Figure E for the B_2 seat. The focus of the validation was good correlation for the x-components of the head, T1, and pelvis accelerations and the y-rotation of the recliner. The MADYMO BioRID I head and T1 x-accelerations, used to calculate NIC_{max} values, showed good correlation to the sled-tests for both crash-pulses. The G_2, B_1, and B_2 seats were not equipped with the same type of head restraint for the two crash pulses in the validation sled-tests, which caused the time discrepancies for the head to head restraint contact with the 4g pulse between the MADYMO simulation and the validation sled-test. The y-rotation of the recliners showed good correlation for all seats.

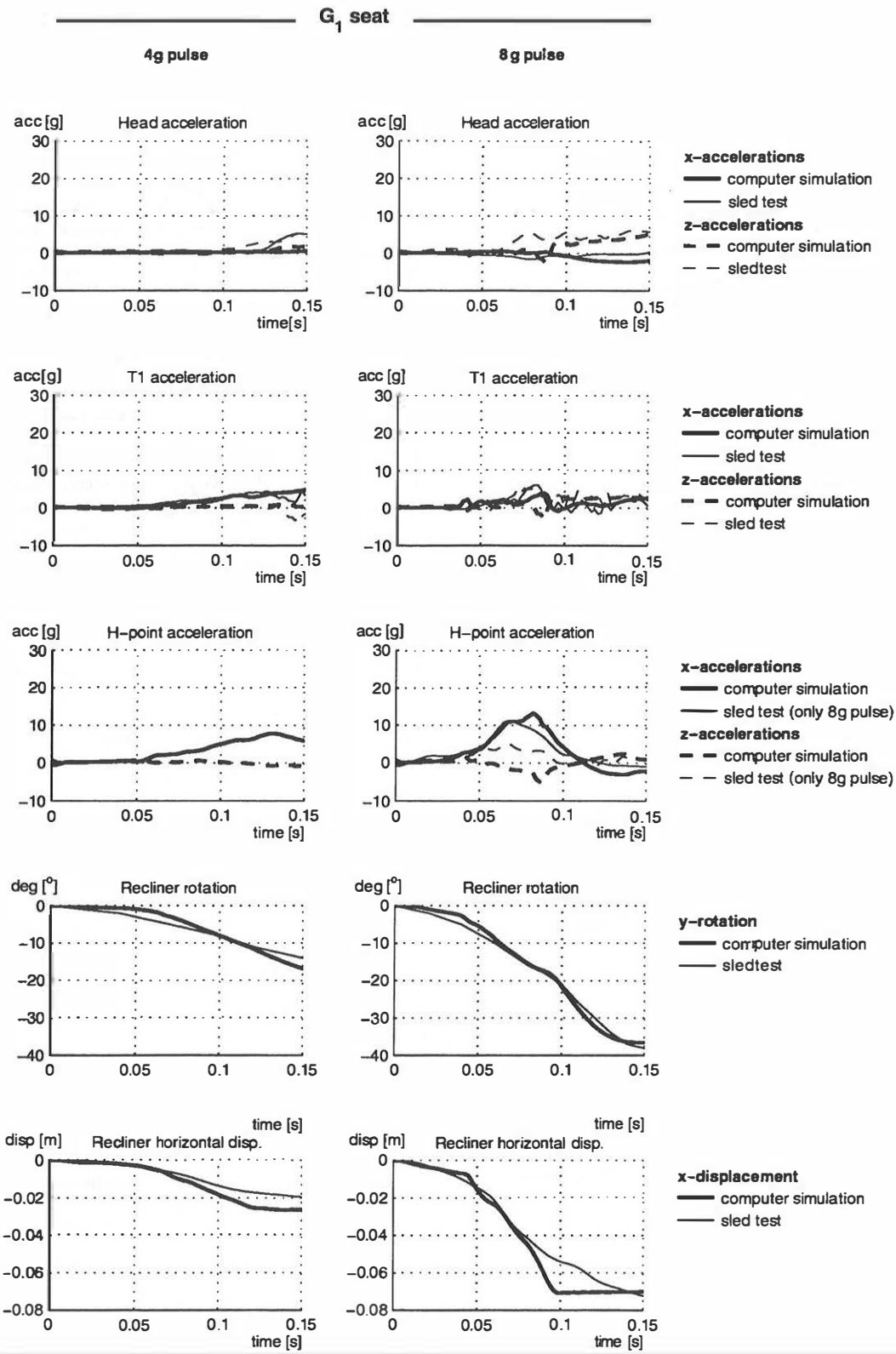

Figure B. Validation results for BioRID I in the G_1 seat.

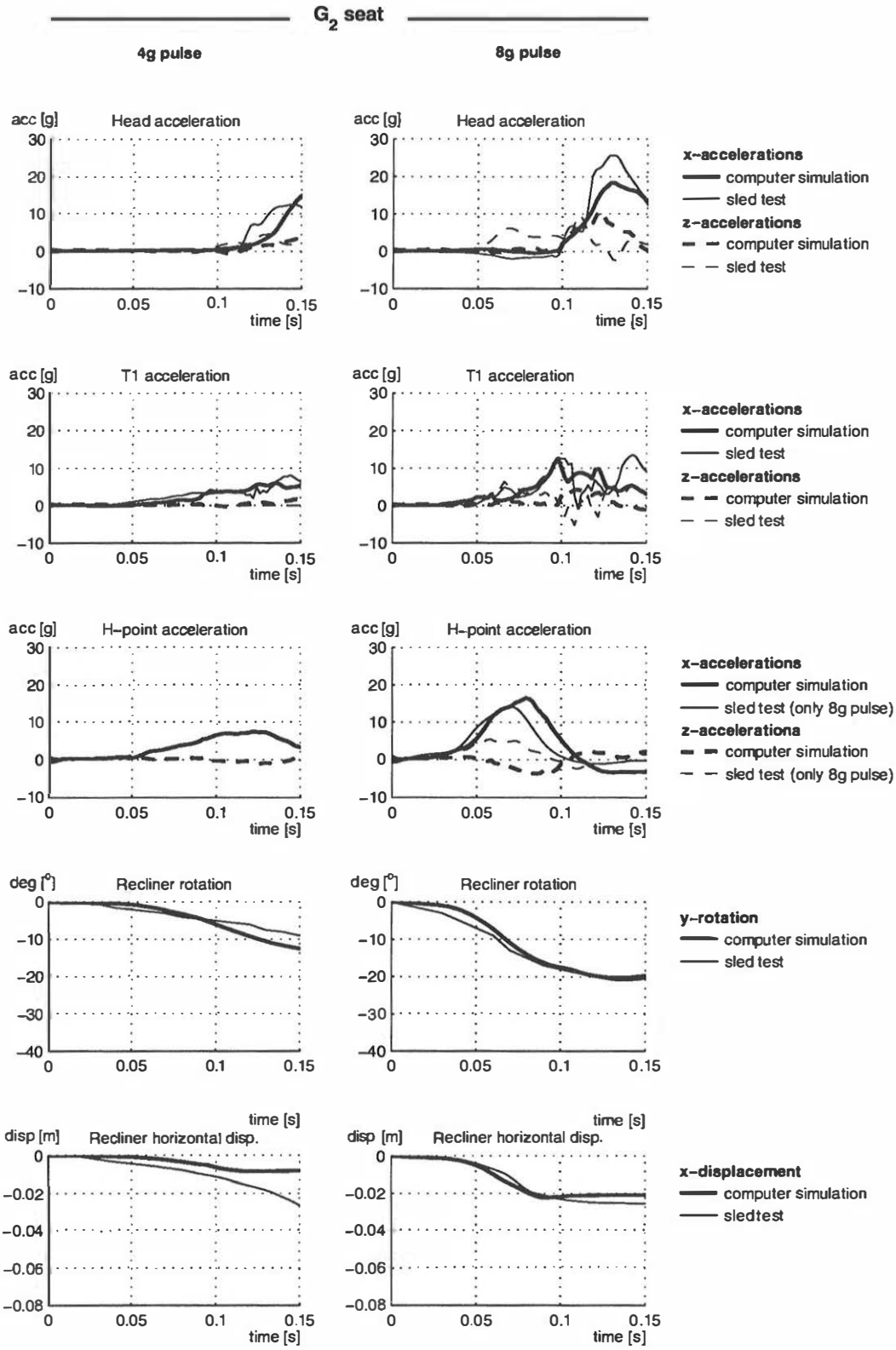

Figure C. Validation results for BioRID I in the G_2 seat.

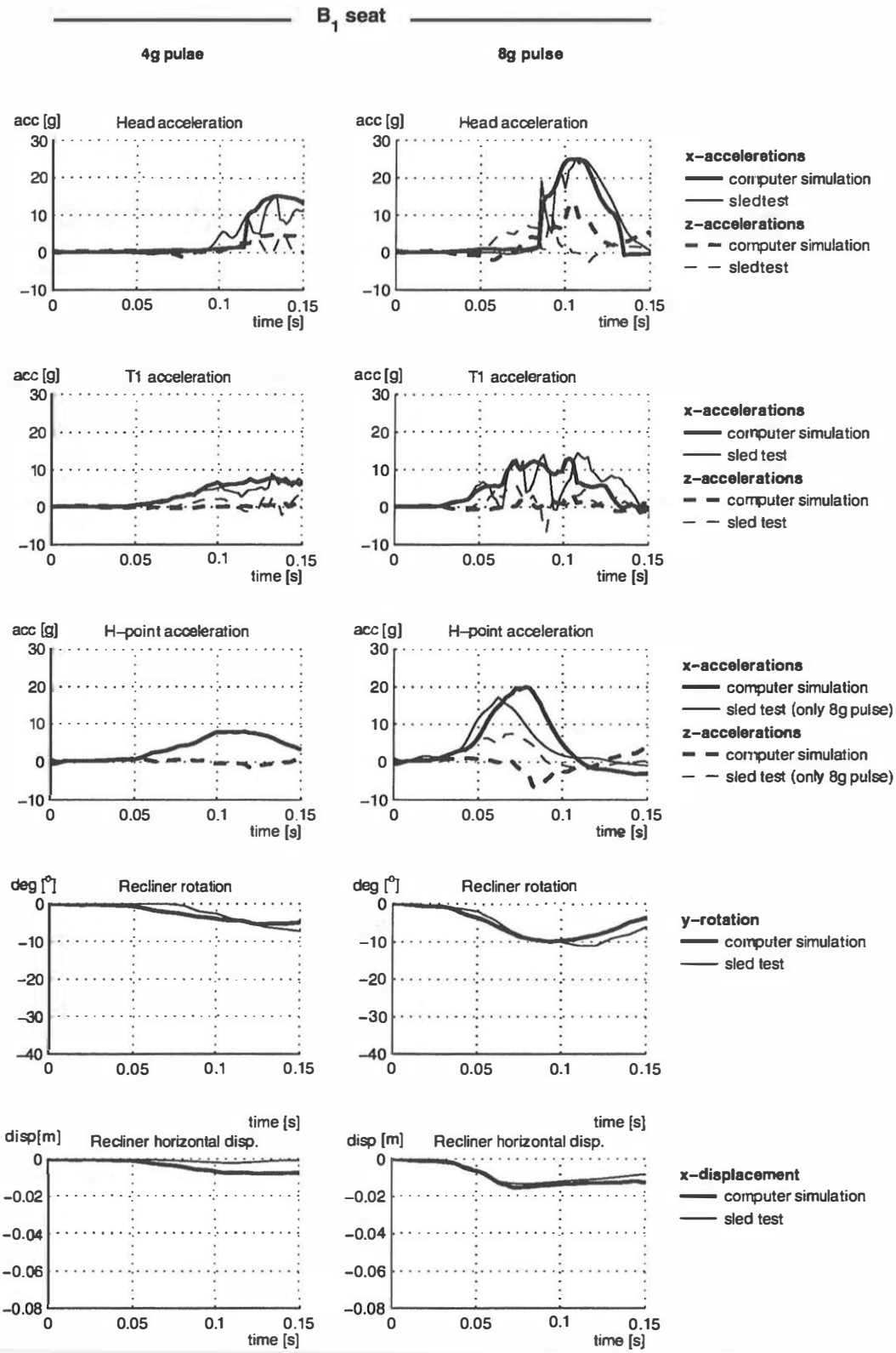

Figure D. Validation results for BioRID I in the B_1 seat.

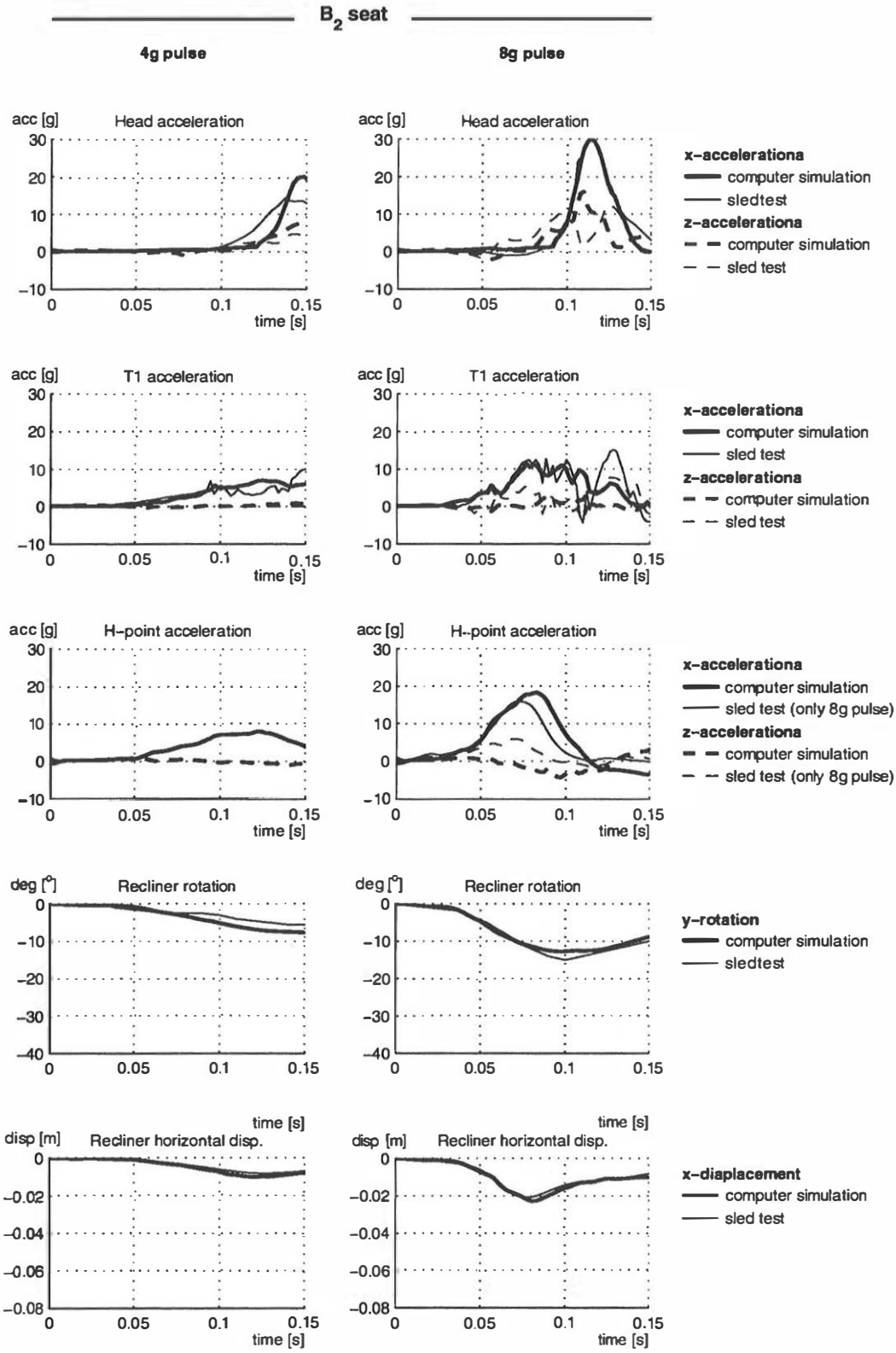

Figure E. Validation results for BioRID I in the B_2 seat.